RSC Advances

PAPER

Pulicaria glutinosa plant extract: a green and eco-friendly reducing agent for the preparation of highly reduced graphene oxide†

Cite this: *RSC Adv.*, 2014, **4**, 24119

Mujeeb Khan,[a] Abdulhadi H. Al-Marri,[a] Merajuddin Khan,[a] Nils Mohri,[b] Syed Farooq Adil,[a] Abdulrahman Al-Warthan,[a] Mohammed Rafiq H. Siddiqui,*[a] Hamad Z. Alkhathlan,[a] Rüdiger Berger,[c] Wolfgang Tremel[b] and Muhammad Nawaz Tahir*[b]

Received 13th February 2014
Accepted 12th May 2014

DOI: 10.1039/c4ra01296h

www.rsc.org/advances

The environmentally friendly synthesis of nanomaterials using green chemistry has attracted tremendous attention in recent years due to its easy handling, low cost, and biocompatibility. Here we demonstrate a facile and efficient route for the synthesis of highly reduced graphene oxide (PE-HRG) by the green reduction of graphene oxide (GRO) using the *Pulicaria glutinosa* plant extract (PE). The phytomolecules present in the *P. glutinosa* extract are not only responsible for the reduction of GRO, but also for the functionalization of the surface of the PE-HRG nanosheets and stabilize them in various solvents, thereby limiting the use of any other external and harmful chemical reductants and surfactants. The effect of PE on the dispersibility of PE-HRG in various solvents was investigated by preparing PE-HRG with different amounts of PE, and the dispersibility of PE-HRG was compared with that of chemically reduced graphene oxide (CRG). The reduction of GRO was confirmed by ultraviolet-visible (UV-vis), Fourier-transform infrared (FT-IR), Raman and X-ray photoelectron (XPS) spectroscopies, thermogravimetric analysis (TGA), X-ray powder diffraction (XRD) and transmission electron microscopy (TEM).

Introduction

Graphene-based materials have been a target for nanotechnologists owing to their exceptionally high crystal and electronic qualities. They have emerged as promising new nanomaterials for a variety of exciting applications despite their short history.[1,2] Due to the stable 2D structure and superior thermal, mechanical and electrical properties,[3–5] graphene is widely used in various fields, including electronics,[6] energy storage,[7] catalysis,[8–11] biosensors[12] and biomedicine.[13,14] Although graphene has been used as a theoretical model to describe the electronic structure of graphitic species for over half a century,[15] researchers have had difficulties in obtaining experimentally relevant amounts of this material until the very recent development of mechanical[16] and chemical synthetic methods.[17–19] Tremendous attention has been paid to the low-cost bulk production of graphene and graphene-based materials,[20–22] for which several methods have been reported. Chemical exfoliation strategies have been applied extensively,[23–25] and sequential oxidation-reduction of graphite and chemical exfoliation of graphite, followed by chemical reduction typically yields flakes of graphene.[26,27] These techniques yield bulk amounts of graphene-like sheets that are best described as highly reduced graphene oxide (HRG).[28,29] This material is not defect free, but highly processable and can be incorporated with a variety of materials, including various graphene-based bio- and nano-composites.[30–32]

The reduction of graphite oxide (GO) or graphene oxide (GRO) to HRG can be performed by chemical,[33–35] thermal,[36] electrochemical[37] and photochemical methods.[38,39] The chemical reduction of GRO is considered the most promising for a large-scale preparation of HRG at a low cost.[40] To date, strong reducing agents such as hydrazine, sodium borohydride, hydroquinone, hydrohalic acid or formamidinesulfinic acid have been applied for the reduction of GRO to HRG.[41–43] However, these chemical reductants, particularly the commonly applied hydrazine, are hazardous and harmful to both human life and the environment. Moreover, the chemical methods may result in "doping" with other elements (nitrogen in the case of hydrazine), which leads to an alteration of the electronic

[a]*Department of Chemistry, College of Science, King Saud University, P. O. Box. 2455, Riyadh, 11451, Kingdom of Saudi Arabia. E-mail: rafiqs@ksu.edu.sa; Fax: +966 1 4676082; Tel: +966 1 4676082*

[b]*Institute of Inorganic and Analytical Chemistry, Johannes Gutenberg-University of Mainz, Mainz, Germany. E-mail: tahir@uni-mainz.de; Fax: +49 6131 3925605; Tel: +49 6131 3925373*

[c]*Max Planck Institute for Polymer Research, Postfach 3148, D-55021 Mainz, Germany*

† Electronic supplementary information (ESI) available: UV spectra and dispersion images of PE-HRG prepared with different concentration of PE and AFM image of PE-HRG. See DOI: 10.1039/c4ra01296h

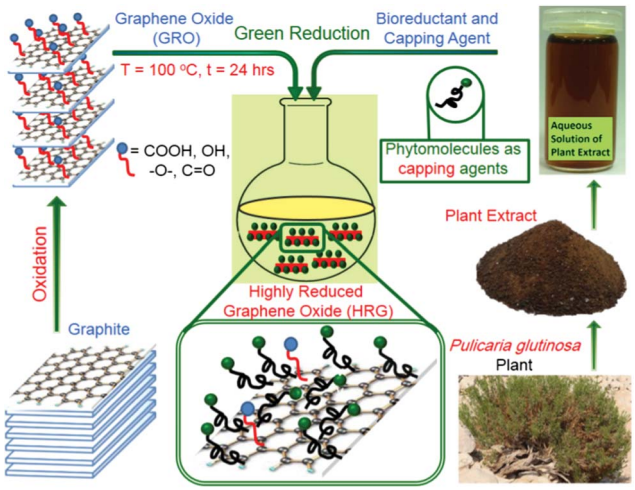

Scheme 1 Green reduction of graphene oxide (GO) using an aqueous extract of the *P. glutinosa* plant.

properties of graphene.[44] Moreover, chemically reduced GRO sheets have a strong tendency to undergo irreversible agglomeration and precipitation due to π–π stacking, which is usually prevented by the addition of chemical stabilizers such as porphyrins, pyrenebutyric acid, or poly(oxyalkylene) amines (POA).[45,46]

Therefore, efforts have been directed towards the development of protocols that make use of eco-friendly reducing agents for the production and stabilization of HRG.[47] To date, some natural products, including gallic acid, L-lysine, melatonine, L-ascorbic acid, green tea, and wild carrot roots, have been explored for the preparation of HRG.[48–53] Recently, the trend of applying plant extracts as both reducing and stabilizing agents during the preparation of nanomaterials has attracted considerable attention.[54,55] Plant extracts (PE) are relatively easy to handle, readily available, low cost, and they have been greatly exploited due to their biocompatibility in the field of nanotechnology.[56,57] Although metal nanoparticles have been synthesized using plant extracts as bioreductants, the reducing abilities of extracts has been rarely tested for the reduction of GO.[58–60]

In this study, we report a facile and environmentally friendly approach for the preparation of highly reduced graphene oxide (HRG) sheets by using an extract from *P. glutinosa* (PE), which has been collected from the local fields in Saudi Arabia (Scheme 1). The PE not only acts as a bioreductant but also functionalizes the surface of the PE-HRG sheets.[60] The as-prepared PE-HRG was characterized using various microscopic and analytical techniques, such as X-ray powder diffraction (XRD), X-ray photoelectron spectroscopy (XPS), Fourier-transform infrared (FT-IR) spectroscopy, Raman spectroscopy, ultraviolet-visible absorption (UV-vis) spectroscopy.

Experimental section

Materials and methods

Graphite powder (99.999%, −200 mesh) was purchased from Alfa Aesar. Concentrated sulfuric acid (H_2SO_4 98%), potassium permanganate ($KMnO_4$ 99%), sodium nitrate ($NaNO_3$, 99%) and hydrogen peroxide (H_2O_2, 30 wt%) and all organic solvents were obtained from Aldrich chemicals and used without further purification.

Synthesis

The whole plant of a wild *P. glutinosa* was collected from a hilly area of Al-Hair in central Saudi Arabia in March 2011. The identity of the plant material was confirmed by a plant taxonomist from the Herbarium Division of the College of Science, King Saud University, Riyadh, Kingdom of Saudi Arabia. A voucher specimen (number KSU-21598) was deposited in our laboratory, as well as in the Herbarium Division of King Saud University. The details of the preparation of the plant extract were given in our previous study.[60] The solution of the plant extract, which was used for the reduction of GRO, was prepared using 0.1 gram of the plant extract in 1 mL of solvent. The chemically reduced graphene oxide (CRG) used in the dispersion studies was obtained by the reduction of GRO using hydrazine hydrate.[61]

Preparation of graphite oxide (GO). Graphite oxide (GO) was synthesized from graphite powder using a modified Hummers method.[62,63] Initially, 2 g of natural graphite and 1.75 g of $NaNO_3$ (purity 99%) were placed in a three-neck flask, to which 150 mL of H_2SO_4 (98%) were added slowly. The mixture was allowed to stir for 2 h in an ice-water bath environment, and after 2 h, 9 g of $KMnO_4$ (99%) were slowly added with constant stirring over a period of 2 h. The remaining mixture was allowed to react for five days at room temperature. Thereafter, 200 mL of 5 wt% H_2SO_4 aqueous solution was added over a period of 1 h and stirred for another 2 h. Afterwards, 6 g of 30 wt% H_2O_2 aqueous solution were added, and the mixture was stirred for another 2 h. The solution was washed several times with an aqueous solution of 3 wt% H_2SO_4 and 0.5 wt% H_2O_2. This process was repeated three times with deionized water (DI). The resulting mixture was dispersed in DI water and centrifuged for 2 h at 9000 rpm. The dispersion was washed 20 times with DI water until a homogeneous brown-black dispersion was obtained.

Preparation of highly reduced graphene oxide (PE-HRG). Graphite oxide or GO (200 mg) was first dispersed in 40 mL of distilled water and sonicated for 30 min to obtain graphene oxide (GRO) sheets. The resulting suspension was heated to 100 °C. Subsequently, 10 mL of an aqueous solution of the plant extract (0.1 g mL^{-1}) was added to the suspension, which was then allowed to stir for 24 h at 98 °C. Subsequently, the highly reduced graphene oxide (PE-HRG-1) was collected by filtration as a black powder, washed with distilled water several times to remove the excess plant extract residue and redistributed into water for sonication. This suspension was centrifuged at 4000 rpm for another 30 min. The final product was collected by vacuum filtration and dried in vacuum.

Characterization

UV/Vis spectroscopy. A Perkin Elmer lambda 35 (USA) UV-vis spectrophotometer was used for the optical measurements. The analysis was performed in quartz cuvettes using DI water as a

reference solvent. Stock solutions of HRG and GRO for the UV measurements were prepared by dispersing 5 mg of sample in 10 mL of DI water and sonicating for 30 min. The UV samples of GRO and PE-HRG were prepared by diluting 1 mL of stock solution with 9 mL of water.

X-ray diffraction. XRD diffractograms were collected on a Altima IV [Make: Rigaku, Japan] X-ray powder diffractometer using Cu Kα radiation ($\lambda = 1.5418$ Å).

Transmission electron microscopy. Transmission electron microscopy (TEM) was performed on a JEOL JEM 1101 (USA) transmission electron microscope. The samples for TEM were prepared by placing a drop of primary sample on a holey carbon copper grid and drying for 6 h at 80 °C in an oven.

Fourier transforms infrared spectrometer. FT-IR spectra were measured on a Perkin-Elmer 1000 (USA) Fourier transforms infrared spectrometer. In order to remove any free biomass residue or unbound extract to the surfaces of PE-HRG sheets, the PE-HRG nanosheets were repeatedly washed with distilled water, and then the product was centrifuged at 9000 rpm for 30 min and dried. The purified PE-HRG nanosheets were mixed with KBr powder and pressed into a pellet for measurement. Background correction was made using a reference blank KBr pellet.

X-ray photoelectron spectroscopy. XPS spectra were measured on a PHI 5600 Multi-Technique XPS (Physical Electronics, Lake Drive East, Chanhassen, MN) using monochromatized Al Kα at 1486.6 eV. Peak fitting was performed using the CASA XPS Version 2.3.14 software.

Atomic force microscopy (AFM). Samples for AFM investigations were prepared by drop casting. One drop of sample solution was deposited on a freshly cleaved mica surface using a 100 μL syringe. Subsequently, the mica sheet was transferred into a high vacuum chamber and dried overnight. All AFM images were recorded using a commercial AFM (Multimode, Nanoscope IIIa controller, Veeco, California, USA) in tapping mode. This instrument was equipped with a piezoelectric scanner allowing a maximum x,y-scan size of 17 μm and a maximum z-extension of 3.9 μm. Silicon cantilevers (OMCL-AC240TS (Olympus), 240 μm long, 30 μm wide, and 2.8 μm thick) with an integrated tip, a nominal spring constant of 2 N m^{-1} and 42 N m^{-1}, a tip radius <10 nm and nominal resonance frequencies of 150 kHz and 450 kHz were plasma-cleaned prior to use.

Results and discussion

P. glutinosa plant extract was used for the synthesis of highly reduced graphene oxide (PE-HRG) as illustrated in Scheme 1. Briefly, plant extract was added to GRO and the contents of the flask were refluxed for 24 h. The color of GRO changed gradually from dark brown to black after the addition of the plant extract (PE), indicating the reduction of GRO. Under a similar set of conditions without the addition of PE, no color change was observed even after 72 hours. The PE-HRG was also compared with chemically reduced graphene oxide (CRG), which was obtained *via* the hydrazine reduction of GRO. To evaluate the effect of the PE concentration on the reduction efficiency of GRO and the surface functionalization of PE-HRG for improving the solubility, three different PE-HRG samples were prepared using 10 mL (PE-HRG-1), 20 mL (PE-HRG-2) and 50 mL (PE-HRG-3) of plant extract at a concentration of 0.1 g mL^{-1} while keeping the amount of GRO constant.

The reduction of GRO was initially monitored by UV-vis spectroscopy as shown in Fig. 1. The GRO shows two characteristic absorption bands at ~230 nm and 301 nm (Fig. 1 red line). Upon chemical reduction (CRG) of GRO with hydrazine both bands vanished, and a new absorption band at ~271 nm appeared (Fig. 1 black line), which also supports the reduction of GRO.[54] Notably, in the case of PE-mediated reduction of GRO (PE-HRG), the absorption peak of the GRO at 230 nm was red shifted to 280 nm (Fig. 1 green line). This shift is considerably higher than that of the chemically reduced GRO (CRG), which exhibited an absorption maximum at 271 nm. This result suggests a higher degree of reduction in the case of PE because the red shift indicates the degree of reduction of GRO.[48]

Moreover, the plant extract mediated reduction product (PE-HRG) showed an extra absorption peak at ~323 nm, (Fig. 1 green line), which is due to the PE phytomolecules bound to the PE-HRG surfaces as confirmed by comparing the absorption spectra of PE-HRG and pure PE (Fig. 1 blue line). The intensity of the absorption band at ~323 nm in PE-HRG (which is the characteristic peak of the PE) increased with increasing concentration of the PE during the reduction of GRO. This clearly indicates that the PE not only reduces GRO, but that the residual phytomolecules of PE functionalize the surface of PE-HRG.

Pristine graphite, GRO, CRG and PE-HRG nanosheets were further characterized by XRD (Fig. 2). The pristine graphite exhibits a very intense and narrow reflection at $2\theta = 26.4°$, corresponding to the (002) planes of the graphene layers with a d spacing of 0.34 nm.[18] However, during the course of the

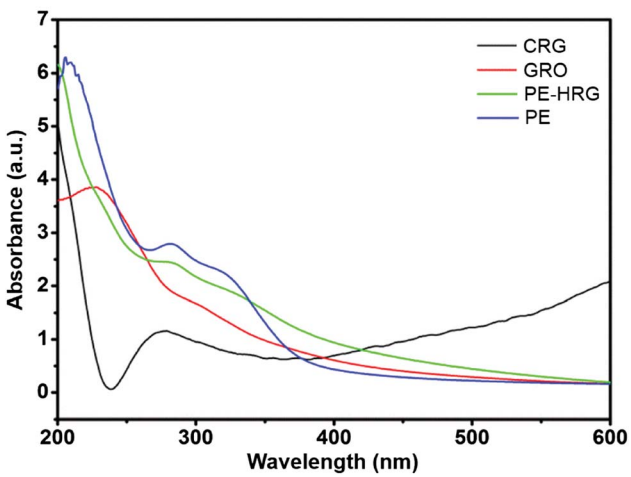

Fig. 1 UV-vis absorption spectra of graphene oxide (GRO, red line), highly reduced graphene oxide (PE-HRG, green line) reduced with PE, chemically reduced graphene oxide (CRG, black line) and pure plant extract (PE, blue line). Although the concentration of CRG was the same as that of RE-HRG, it exhibits a much lower absorption coefficient due to its poor dispersibility in water.

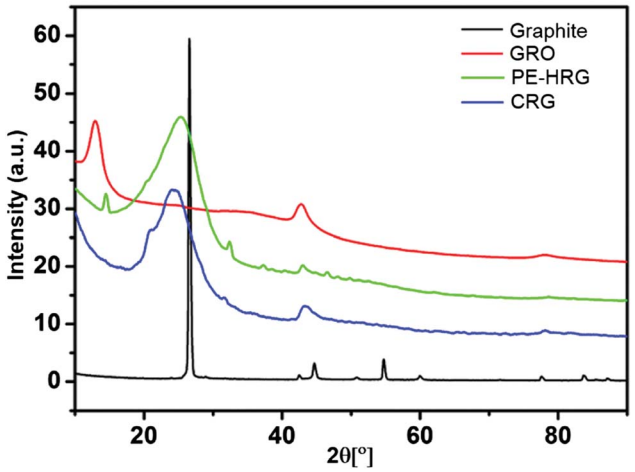

Fig. 2 XRD diffractograms of graphite, graphene oxide (GRO), PE mediated highly reduced graphene oxide (PE-HRG) and chemically reduced graphene oxide (CRG).

oxidation, various oxygen containing functional groups were incorporated between the carbon nanosheets, leading to a shift in the GRO reflection to a lower Bragg angle ($2\theta = 10.9°$). Apart from the functional groups, a large number of water molecules were intercalated between the layers. As a result, the *d* spacing of GRO increased to 0.79 nm, which is almost twice as high as the *d* spacing of pristine graphite (0.34 nm). However, the reflection of GRO at 10.9° disappeared in HRG after the reduction, which suggests that the oxygen-containing functional groups were essentially removed. Moreover, a broad reflection centered at $2\theta = 22.4°$ in the diffraction pattern of PE-HRG indicates the formation of graphene nanosheets with a thickness of a few layers.[23]

The FT-IR spectrum of GRO contains several bands that indicate the presence of oxygen-containing moieties like carbonyl, carboxylic, epoxy and hydroxyl groups (Fig. 3).[26,43] The reduced intensities of the bands at 1985, 1727, 1605, 1234 and 1047 cm^{-1} associated with these oxygen containing functional groups indicate the reduction of the GRO, *i.e.* the number of oxygen-containing functional groups decreased significantly after the reduction (Fig. 3).

However, some of the bands observed in the spectrum of PE-HRG could be due to the presence of phytomolecules bound following the *in situ* functionalization. This was confirmed by a comparison of the IR spectra of PE-HRG and the pure plant extract (Fig. 3). Most of the absorption bands due to PE also appear in the FT-IR spectrum of PE-HRG. This strongly suggests that the phytomolecules of PE act not only as bioreductants, but also act as stabilizers by adsorbing on the HRG sheets. Notably, the absence of absorption bands at 1392 cm^{-1} and 1270 cm^{-1} associated with the phenolic OH groups in the FT-IR spectrum of PE-HRG (present in the spectrum of PE due to phenolic OH) suggest that a possible reduction of GRO is carried out by the phenolic OH groups.

The reduction of GRO was monitored by thermal analysis. The TGA traces of pure graphite, pure PE, GRO, PE-HRG and CRG are shown in Fig. 4. Graphite did not show any weight loss (Fig. 4 black line), whereas several degradation steps were observed for GRO (Fig. 4 red line). Initially, ~15% weight loss at about 110 °C, may be assigned to the loss of adsorbed water, followed by another steep step (weight loss ~25%) at ~200 °C, which was assigned to the thermal elimination of labile oxygen-containing functional groups (hydroxyl or epoxy). A gradual weight loss of ~20% was observed in the temperature range from 200–800 °C. The total residual weight of GRO obtained at 800 °C was around 40%.[38,48]

CRG exhibited no weight loss up to 250 °C; however, in the temperature range of 250–800 °C, CRG exhibited a weight loss of ~15% (Fig. 4 blue line). The PE-HRG showed less weight loss around 200 °C compared to GRO, but a total weight loss of ~30% between 500 °C and 800 °C, which could be due to the PE bound to the surface of PE-HRG (Fig. 4 green line). This result

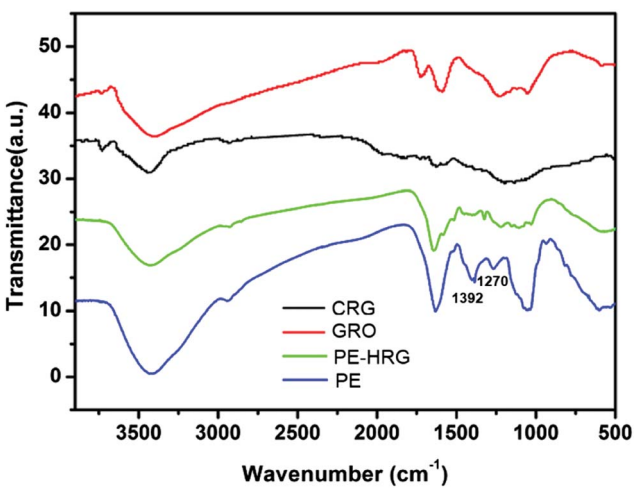

Fig. 3 FT-IR spectra of graphene oxide (GRO), PE-mediated highly reduced graphene oxide (PE-HRG), and chemically reduced graphene oxide (CRG) prepared with hydrazine hydrate and the plant extract (PE).

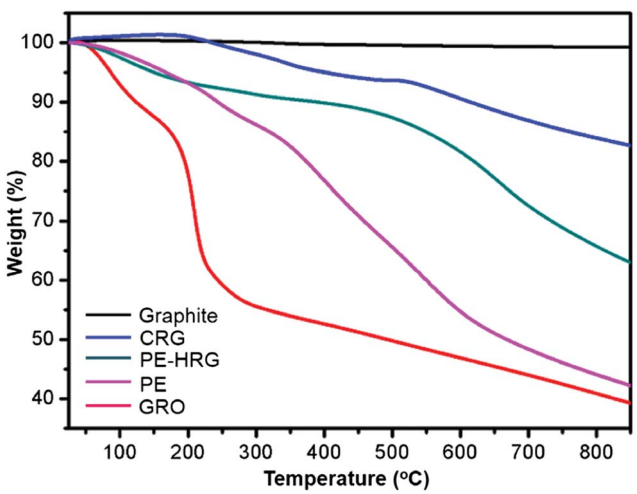

Fig. 4 TGA traces of pure graphite, plant extract (PE), graphene oxide (GRO), chemically reduced graphene oxide (CRG) and highly reduced graphene oxide (PE-HRG) obtained using the plant extract.

was confirmed by the TGA trace of the pure PE (Fig. 4 pink line), which also showed the same trend, presumably due to the PE extract bound to the surfaces. The residual weight obtained after annealing CRG and PE-HRG was about 85% and 70% at 800 °C, respectively (Fig. 4).[50] The higher weight loss for PE-HRG (30%) compared to CRG (15%) can be assigned to the surface-bound phytomolecules.

Raman spectroscopy was used to characterize GRO and PE-HRG.[41] The Raman spectra of graphene contain two main features: the G and D bands, which are observed at 1575 cm^{-1} and 1350 cm^{-1}, respectively.[50] The G and the D bands of GO are shifted and appear at 1592 and 1346 cm^{-1} (Fig. 5 red line), respectively, due to the destruction of the sp^2 character and the formation of defects in the sheets caused by the extensive oxidation. After the reduction, the G band of PE-HRG is slightly narrower and shifted to 1582 cm^{-1}, while the D band is at 1343 cm^{-1} (Fig. 5 black line). A comparison of the Raman spectra of both GO and PE-HRG showed that the G band of PE-HRG had shifted by 10 cm^{-1} from 1592 to 1582 cm^{-1}, whereas only a slight shift was observed in the D band from 1346 to 1343 cm^{-1}. The shift in the bands of PE-HRG after the reduction towards the ideal positions of the G band (1575 cm^{-1}) and D band (1350 cm^{-1}) of graphene is a clear indication of the restoration of the sp^2 character of PE-HRG, and it is compatible with a high degree of reduction.

XPS can provide valuable information regarding the behavior of oxygen-containing functional groups on the carbon skeleton. In order to demonstrate the reduction of GRO by PE, high resolution C1s spectra of GRO and PE-HRG were obtained (Fig. 6). The C1s spectrum of GRO displayed four different kinds of signals, which were assigned to the C–C bonding of the sp^2 carbon of the graphitic structure and the oxygen-containing functional groups attached to the surface of the GRO due to the oxidation of graphite (*e.g.* hydroxyl, epoxy, alkoxy and carbonyl (C–O, C═O, O–C═O)). The C1s signals observed at 284.7, 286.9, 288.3 and 289.1 eV are attributed to the sp^2 carbon C–C, C–O, C═O, and O–C═O groups of GRO, respectively. Peak fitting

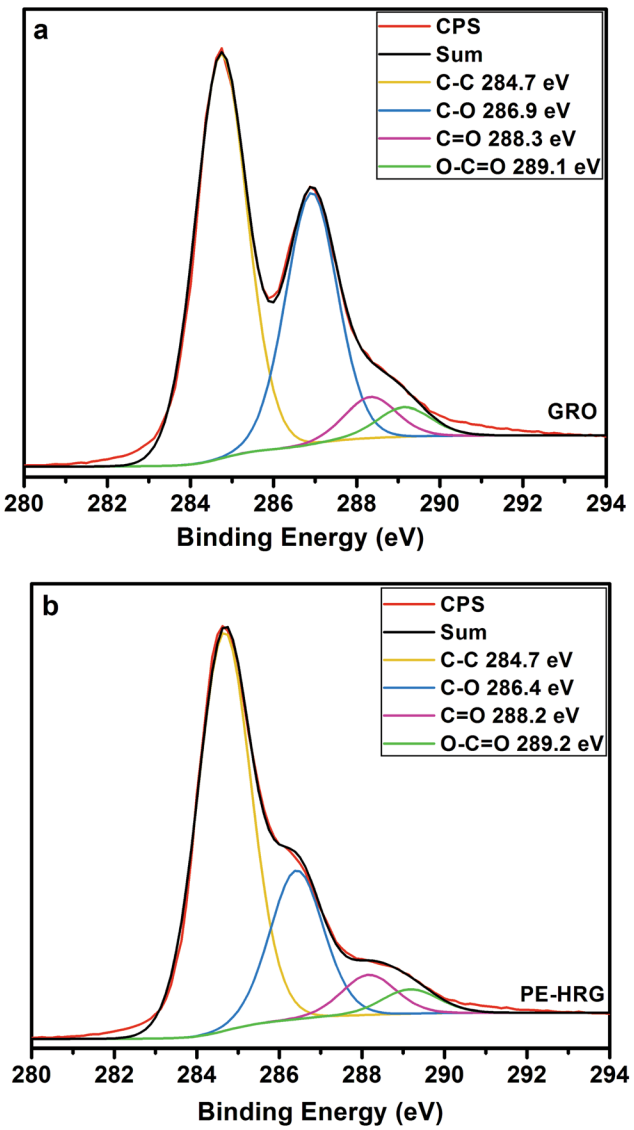

Fig. 6 XPS spectra of (top) GRO and (bottom) PE-HRG showing the partial removal of oxygen-containing functional groups from the surface of the GRO.

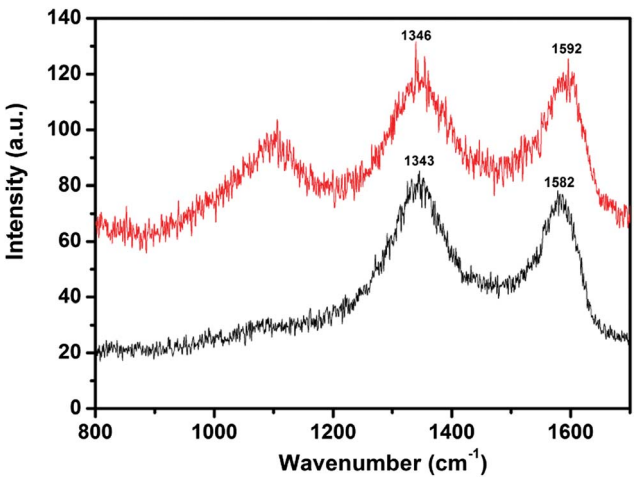

Fig. 5 Raman spectra of graphene oxide (GRO, red line) and highly reduced graphene oxide (PE-HRG, black line) using plant extract.

resulted in atomic concentrations of 55.58%, 34.57%, 5.62% and 4.23% for the different groups. Although similar signals also appeared at almost the same positions for PE-HRG-1 after the reduction, the intensities of the signals belonging to the oxygen containing functional groups (286.4, 288.2 and 289.2 eV) were much lower (Fig. 6b bottom), which suggests that the number of oxidized groups on the surface of the GRO sheets decreased significantly after the reduction. Peak fitting resulted in atomic concentrations of 65.04%, 24.24%, 6.54% and 4.17% for the different groups. It is worth mentioning that despite a decrease in the intensity of the peaks corresponding to oxygen functional groups, the elemental (C/O) ratio in PE-HRG is not as high as that reported for the chemically reduced graphene or bio-reduced without a stabilizer.[50] This observation could be due to the fact that the PE molecules are also bound to the PE-HRG surfaces (as indicated by UV-vis and FT-IR data) and

contribute to the presence of an extra amount of oxygen. Similar results were also obtained by Yan *et al.* using gallic acid as a reducing and stabilizing agent.[48]

The morphology and layer thickness of the PE-HRG were determined by TEM and AFM (Fig. 7). The TEM images (Fig. 7a and b) revealed the transparent and sheet-like structure of PE-HRG. A large number of wrinkles and scrolls were observed on the surface of the PE-HRG sheet, which remained stable under the high energy electron beam. We observed that the edges of the suspended graphene layers were folded back, and there was also a formation of a few graphene layers in the high resolution TEM. The AFM height profile obtained at 3 different locations (Fig. 7c) showed a maximum thickness ~3.3 nm, indicating the presence of 3–4 layers thick sheets and the smallest step height was measured to be 0.9 nm (Fig. S1†), which we associate with a single graphene layer situated directly on the mica substrate.[64]

The formation of stable and homogeneous graphene suspensions in different solvents is a formidable challenge, which is met with external surfactants or stabilizers including polymers or nanoparticles.[45,48] The bio-reduction of GRO generally avoids the addition of any other surfactant to obtain stable solutions of graphene-type materials. As the role of the *P. glutinosa* PE as a bioreductant and stabilizer was confirmed by our previous results,[60,65] we investigated the dispersibility of the bio-reduced PE-HRG and compared it with that of CRG. For this purpose, freshly produced PE-HRG-1, PE-HRG-2 (Fig. S2†) and PE-HRG-3 prepared with different amounts of PE (10, 20 and 50 mL), respectively, as well as CRG, were dispersed in DI water and other organic solvents (acetone, ethanol, DMSO and DMF, see Fig. 8). The dispersions were prepared by sonicating 5 mg of CRG or PE-HRG in 10 mL of solvent. Superior dispersions were obtained for the bio-reduced PE-HRG as compared to CRG. The dispersion quality of PE-HRG was enhanced by increasing the amount of PE. Fig. 8 compares the dispersibility of PE-HRG-3 and CRG in five different solvents. After two weeks, the CRG suspensions had become unstable, whereas PE-HRG-3 still exhibited excellent dispersibility in most solvents.

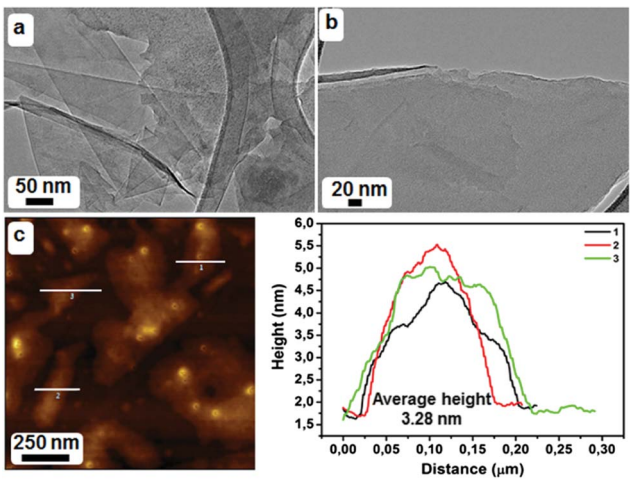

Fig. 7 TEM images (a and b) of as-prepared PE-HRG at different resolutions, (c) AFM height image of PE-HRG with the corresponding line profiles.

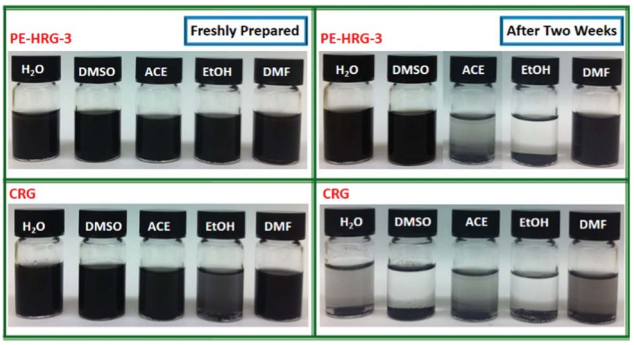

Fig. 8 Digital images of the dispersions of PE-HRG-3 (prepared with 50 mL of plant extract) and CRG (prepared with hydrazine hydrate).

Conclusions

In summary, we describe a green and eco-friendly method for the reduction of GRO with *P. glutinosa* PE, which not only acts as a bioreductant but also acts as a stabilizer. Spectroscopic, diffraction and imaging techniques confirmed the partial reduction of GRO to PE-HRG, whereas TEM and AFM indicated the presence of multiple layers of graphene (PE-HRG) in the product. The bio-reduced PE-HRGs exhibited an enhanced dispersibility in various solvents compared to chemically reduced graphene (CRG). The quality and dispersion stability of PE-HRG was improved significantly with increasing amount of PE. The bio-reduction in the presence of the *P. glutinosa* extract appears to be a useful substitute for conventional reduction methods in the synthesis of highly reduced graphene oxide (HRG). The abundance, easy collection and low cost of *P. glutinosa* plant extracts makes it potentially attractive for the large-scale synthesis of graphene and other graphene-based materials.

Acknowledgements

This project was supported by NSTIP Strategic technologies programs, number (11NAN1860-02) in the Kingdom of Saudi Arabia

Notes and references

1 A. K. Geim and K. S. Novoselov, *Nat. Mater.*, 2007, **6**, 183–191.
2 K. S. Novoselov, V. I. Falko, L. Colombo, P. R. Gellert, M. G. Schwab and K. Kim, *Nature*, 2012, **490**, 192–200.
3 J. K. Wassei and R. B. Kaner, *Acc. Chem. Res.*, 2013, **10**, 2244–2253.
4 O. V. Yazyev, *Acc. Chem. Res.*, 2013, **10**, 2319–2328.
5 Y. Chen, B. Zhang, G. Liu, X. Zhuang and E. T. Kang, *Chem. Soc. Rev.*, 2012, **41**, 4688–4707.
6 X. Wan, Y. Huang and Y. Chen, *Acc. Chem. Res.*, 2012, **45**, 598–607.
7 W. Qian, Z. Chen, S. Cottingham, W. A. Merill, N. A. Swartz, A. M. Goforth, T. L. Clare and J. Jiao, *Green Chem.*, 2012, **14**, 371–377.

8 H. Wang, T. Deng, Y. Wang, X. Cui, Y. Qi, X. Mu, X. Hou and Y. Zhu, *Green Chem.*, 2013, **15**, 2379–2383.
9 P. P. Upare, J. W. Yoon, M. Y. Kim, H. Y. Kang, D. W. Hwang, Y. K. Hwang, H. H. Kung and J. S. Chang, *Green Chem.*, 2013, **15**, 2395–2943.
10 D. He, Z. Kou, Y. Xiong, K. Cheng, X. Chen, M. Pan and M. Schichun, *Carbon*, 2014, **66**, 312–319.
11 H. Huang, J. Huang, Y. M. Liu, H. Y. He, Y. Cao and K. N. Fan, *Green Chem.*, 2012, **14**, 930–934.
12 R. Hernandez, C. Valles, A. M. Benito, W. K. Maser, F. X. Rius and J. Riu, *Biosens. Bioelectron.*, 2014, **54**, 553–557.
13 K. Yang, L. Feng, X. Shi and Z. Liu, *Chem. Soc. Rev.*, 2013, **42**, 530–547.
14 H. Zhou, B. Zhang, J. Zheng, M. Yu, T. Zhou, K. Zhao, Y. Jia, X. Gao, C. Chen and T. Wei, *Biomaterials*, 2014, **35**, 1597–1607.
15 J. C. Slonczewski and P. R. Weiss, *Phys. Rev.*, 1958, **109**, 272–279.
16 K. S. Novoselov, A. K. Geim, S. V. Morozov, D. Jiang, Y. Zhang, S. V. Dubonos, I. V. Grigorieva and A. A. Firsov, *Science*, 2004, **306**, 666–669.
17 S. Park and R. S. Ruoff, *Nat. Nanotechnol.*, 2009, **4**, 217–224.
18 C. K. Chua and M. Pumera, *Chem. Soc. Rev.*, 2014, **43**, 291–312.
19 A. Ciesielski and P. Samori, *Chem. Soc. Rev.*, 2014, **43**, 381–398.
20 R. S. Edwards and K. S. Coleman, *Nanoscale*, 2013, **5**, 38–51.
21 N. Mahmood, C. Zhang, H. Yin and Y. Hou, *J. Mater. Chem. A*, 2014, **2**, 15–32.
22 S. Bai and X. Shen, *RSC Adv.*, 2012, **2**, 64–98.
23 T. Kuila, A. K. Mishra, P. Khanra, N. M. Kim and J. H. Lee, *Nanoscale*, 2013, **5**, 52–71.
24 A. Martin, J. H. Ferrer, L. Vazquez, M. T. Martinez and A. Escarpa, *RSC Adv.*, 2014, **4**, 132–139.
25 J. W. Ko, S.-W. Kim, J. Hong, J. Ryu, K. Kang and C. B. Park, *Green Chem.*, 2012, **14**, 2391–2394.
26 D. R. Dreyer, S. Park, C. W. Bielawski and R. S. Ruoff, *Chem. Soc. Rev.*, 2010, **39**, 228–240.
27 W. Gao, L. B. Alemany, L. J. Ci and P. M. Ajayan, *Nat. Chem.*, 2009, **1**, 403–408.
28 H. Feng, R. Cheng, X. Zhao, X. Duan and J. Li, *Nat. Commun.*, 2013, **4**, 1539.
29 K. Moonl, J. Lee, R. S. Ruoff and H. Lee, *Nat. Commun.*, 2010, **1**, 73–79.
30 W. Yue, S. Jiang, W. Huang, Z. Gao, J. Li, Y. Ren, X. Zhao and X. Yang, *J. Mater. Chem. A*, 2013, **1**, 6928–6933.
31 L. Wang, X. Lu, S. Lei and Y. Song, *J. Mater. Chem. A*, 2014, **2**, 4491–4509.
32 G. Long, C. Tang, K. Wong, C. Man, M. Fan, W. Lau, T. Xu and B. Wang, *Green Chem.*, 2013, **15**, 821–828.
33 N. H. Kim, T. Kuila and J. H. Lee, *J. Mater. Chem. A*, 2013, **1**, 1349–1358.
34 L. Wang, Y. Park, P. Cui, S. Bak, H. Lee, S. M. Lee and H. Lee, *Chem. Commun.*, 2014, **50**, 1224–1226.
35 A. K. Das, M. Srivastav, R. K. Layek, M. E. Uddin, D. Jung, N. H. Kim and J. H. Lee, *J. Mater. Chem. A*, 2014, **2**, 1332–1340.
36 Z. G. Wang, P. J. Li, Y. F. Chen, J. R. He, B. J. Zheng, J. B. Liu and F. Qi, *Mater. Lett.*, 2014, **116**, 416–419.
37 Y. Li, K. Sheng, W. Yuan and G. Shi, *Chem. Commun.*, 2013, **49**, 291–293.
38 R. Y. N. Gengler, D. S. Badali, D. Zhang, K. Dimos, K. Spyrou, D. Gourins and R. J. D. Miller, *Nat. Commun.*, 2013, **4**, 2560–2565.
39 Y. Pan, S. Wang, C. W. Kee, E. Dubuisson, Y. Yang, K. P. Loh and C. H. Tan, *Green Chem.*, 2011, **13**, 3341–3344.
40 O. C. Compton and S. B. Nguyen, *Small*, 2010, **6**, 711–723.
41 X. Gao, J. Jang and S. Nagase, *J. Phys. Chem. C*, 2010, **114**, 832–842.
42 H. J. Shin, K. K. Kim, A. Benayad, S. M. Yoon, H. K. Park, I. S. Jung, M. H. Jin, H. K. Jeong, J. M. Kim, J. Y. Choi and Y. H. Lee, *Adv. Funct. Mater.*, 2009, **19**, 1987–1992.
43 S. Pei, J. Zhao, J. Du, W. Ren and H. M. Cheng, *Carbon*, 2010, **48**, 4466–4474.
44 D. Luo, G. Zhang, J. Liu and X. Sun, *J. Phys. Chem. C*, 2011, **115**, 11327–11335.
45 M. Quintana, E. Vazquez and M. Prato, *Acc. Chem. Res.*, 2013, **46**, 138–148.
46 T. Kuila, S. Bose, A. K. Mishra, P. Khanra, N. H. Kim and J. H. Lee, *Prog. Mater. Sci.*, 2012, **57**, 1061–1105.
47 Y. Lei, Z. Tang, R. Liao and B. Guo, *Green Chem.*, 2011, **13**, 1655–1658.
48 J. Li, G. Xiao, C. Chen, R. Li and D. Yan, *J. Mater. Chem. A*, 2013, **1**, 1481–1487.
49 Y. Guo, S. Guo, J. Ren, Y. Zhai, S. Dong and E. Wang, *ACS Nano*, 2010, **4**, 4001–4010.
50 T. Kuila, S. Bose, P. Khanra, A. K. Mishra, N. H. Kim and J. H. Lee, *Carbon*, 2012, **50**, 914–921.
51 J. Zhang, H. Yang, G. Shen, P. Cheng, J. Zhang and S. Guo, *Chem. Commun.*, 2010, **46**, 1112–1114.
52 H. L. Guo, X. F. Wang, Q. Y. Qian, F. B. Wang and X. H. Xia, *ACS Nano*, 2009, **3**, 2653–2659.
53 C. Zhu, S. Guo, Y. Fang and S. Dong, *ACS Nano*, 2010, **4**, 2429–2437.
54 S. Irvani, *Green Chem.*, 2011, **13**, 2638–2650.
55 M. S. Akther, J. Panwar and Y. S. Yun, *ACS Sustainable Chem. Eng.*, 2013, **1**, 591–602.
56 A. K. Mittal, Y. Chisti and U. C. Banerjee, *Biotechnol. Adv.*, 2013, **31**, 346–356.
57 B. Haghighi and M. A. Tabrizi, *RSC Adv.*, 2013, **3**, 13365–13371.
58 S. Thakur and N. Karak, *Carbon*, 2012, **50**, 5331–5339.
59 D. Mhamane, W. Ramadan, M. Fawzy, A. Rana, M. Dubey, C. Rode, B. Lefez, B. Hannoyer and S. Ogale, *Green Chem.*, 2011, **13**, 1990–1996.
60 M. Khan, M. Khan, S. F. Adil, M. N. Tahir, W. Tremel, H. Z. Alkhathlan, A. Al-Warthan and M. R. H. Siddiqui, *Int. J. Nanomed.*, 2013, **8**, 1–10.
61 Q. Cheng, J. Tang, J. Ma, H. Zhang, N. Shinya and L. C. Qin, *Carbon*, 2011, **49**, 2917–2925.
62 W. S. Hummers and R. E. Offeman, *J. Am. Chem. Soc.*, 1958, **80**, 1339.
63 L. Ji, Z. Tan, T. R. Kuykendall, S. Aloni, S. Xun, E. Lin and V. B. Y. Zhang, *Phys. Chem. Chem. Phys.*, 2011, **13**, 7170–7177.
64 A. Gupta, G. Chen, P. Joshi, S. Tadigadapa and P. C. Eklund, *Nano Lett.*, 2006, **6**, 2667–2673.
65 M. Khan, M. Khan, M. Kuniyil, S. F. Adil, A. Al-Warthan, H. Z. Alkhathlan, W. Tremel, M. N. Tahir and M. R. H. Siddiqui, *Dalton Trans.*, 2014, **43**, 9026–9031.